Materials Letters 145 (2015) 355–358

Contents lists available at ScienceDirect

Materials Letters

journal homepage: www.elsevier.com/locate/matlet

Novel SnO_2 ceramic surge absorbers for low voltage applications

M. Maleki Shahraki [a], M.A. Bahrevar [a,*], S.M.S. Mirghafourian [b], A.B. Glot [c]

[a] Materials and Energy Research Center, Semiconductors Department, PO Box 14155-4777, Karaj, Iran
[b] Pars Electrical Transmission Equipment Company, PO Box 81395-178, Esfahan, Iran
[c] Universidad Tecnologica de la Mixteca, Huajuapan de Leon, Oaxaca 69000, Oaxaca, Mexico

ARTICLE INFO

Article history:
Received 22 December 2014
Accepted 28 January 2015
Available online 7 February 2015

Keywords:
Varistor
Tin oxide
Electrical properties
Low voltage application
Surge-withstand capability

ABSTRACT

To make SnO_2–CoO–Nb_2O_5–Cr_2O_3–Y_2O_3–Bi_2O_3 ceramics suitable for low voltage varistor applications, the amount of Bi_2O_3 addition to a well-known SnO_2-based composition for high voltage varistors was optimized. The addition of 0.15 mol% Bi_2O_3 has resulted in a single phase ceramic material with the average grain size of 30 μm and electrical properties useful for low voltage varistors. The obtained SnO_2 low voltage varistors exhibit excellent electrical properties as surge absorbers.

1. Introduction

Commercial varistors (surge arrestors for high-voltage applications and surge absorbers for low-voltage applications) are mainly based on zinc oxide [1]. ZnO varistors suffer from a number of drawbacks; namely, the multitude of additives, inhomogeneous multi-phase microstructure, and the degradation phenomenon [2,3]. In order to overcome the above-mentioned drawbacks, new metal-oxide varistors based on SnO_2 are currently being developed [4,5]. Due to their simpler microstructure, higher breakdown field, higher thermal conductivity, and better degradation behavior, SnO_2 varistors have already been considered as promising substitutes for high voltage ZnO varistors [5,6]. The 98.9 mol%SnO_2–1 mol%CoO–0.05 mol%Nb_2O_5–0.05 mol%Cr_2O_3 is a well-known varistor composition with a high nonlinear coefficient (α=41), breakdown field (E_b=4 kV/cm) [7]. The addition of Y_2O_3 to this system is reported to cause the withstanding surge current density to increase up to 2600 A/cm^2 [8] which is still far below that of high voltage ZnO varistors. In contrast, the withstanding surge current density of low voltage commercial ZnO varistors lies in the range of 0.5–2.0 kA/cm^2, comparable to that of high voltage (Co, Nb, Cr, Y)-doped SnO_2 varistor.

Electrical behavior of SnO_2 ceramics can be tailored to suit low voltage applications similarly to ZnO varistors whilst keeping their other superior properties provided that the SnO_2 grain size can be increased either with the adoption of a refined processing regime or the right choice of additives [9]. Their surge-withstand capability could also be acceptable. However, very few reports on the low voltage SnO_2-based varistors have been published so far [10,11]. Low α values ($\leq$10) have been reported for coarse-grained SnO_2 varistors made through modifying the sintering process and scarce electrical data is available in the upturn region [10–12]. It has been reported that Bi_2O_3 is an effective additive for the grain growth with no deleterious effect on electrical properties of (Co, Nb)-doped SnO_2 varistor [13]. Recently, we reported that the addition of Bi_2O_3 (0.5 mol%) to SnO_2 with small amounts of Nb_2O_5 and Cr_2O_3 (0.05 mol%) gives ceramic material for low voltage varistors [14].

In this research, novel low voltage SnO_2-based varistors are developed through adding various amounts of Bi_2O_3 to the (Co, Nb, Cr, Y)-doped SnO_2 system. The composition has been optimized to yield the best electrical properties of the SnO_2 based surge absorber.

2. Experimental

The varistor molar composition was (97.35-x)% SnO_2+ 2.5% CoO+ 0.05% Nb_2O_5+ 0.05% Cr_2O_3 + 0.05% Y_2O_3+x%Bi_2O_3, with x=0, 0.05, 0.15, and 0.45. Varistor compositions were labeled as SCNCrY-xBi with x denoting the various amounts of Bi_2O_3. Apart from Nb_2O_5, all the oxides in this study were nano-sized (50–100 nm) and had a purity of at least 99.5%. A high energy mill (SPEX-8000) was employed to grind Nb_2O_5 separately. The specific surface area of the milled powder was about 15 m^2/g. All the nano-sized precursor powders were wet milled. PVA was added as a binder for granulation. The granulated powder was then pressed into pellets of 1 mm thick under axial pressure of 200 MPa. After

* Corresponding author. Tel.: +98 9121055493.
E-mail address: ma.bahrevar@yahoo.com (M.A. Bahrevar).

http://dx.doi.org/10.1016/j.matlet.2015.01.148
0167-577X/

burning out the organic binder, samples were sintered in a two-stage regime. They were slowly heated up to 1300 °C, then they were kept at this temperature during 2.5 h, then temperature was increased to 1350 °C and samples were soaked at 1350 °C during 2.5 h and, finally, they were slowly cooled down. The density was determined using Archimedes method. The X-ray diffraction (XRD) analysis was carried out using Philips Xpert 3710 diffractometer with Co-K_α radiation ($\lambda = 1.789$ A). A precise XRD pattern was obtained by choosing a step of 0.01° with duration of 10 s per step. The TESCAN scanning electron microscope was employed to acquire the micrographs of polished and thermally etched samples. The average grain size was determined using Mendelson method.

For the electrical measurements, silver paste electrodes were screen printed on the flat surfaces of samples and fired for 15 min at 600 °C. The *J*–*E* characteristics in the pre-breakdown and non-ohmic region were measured using a Keithley 2410 source meter. The breakdown electric field, E_b, was determined at a current density of 1 mA/cm^2. The leakage current (I_L) was measured at 0.8 E_b. The nonlinearity coefficient α, was calculated using equation:

$$\alpha = \frac{1}{\left(\log E_{10\ \mathrm{mA/cm^2}}/E_{1\ \mathrm{mA/cm^2}}\right)} \quad (1)$$

To evaluate the upturn part of the *J*–*E* curve, the high current impulse tests were performed. For such tests the current generator delivering 8/20 μs impulse current was used. The varistor response was recorded using Rigol DS5022M digital storage oscilloscope. The withstanding surge current density was defined as the maximum peak current density if a variation of the varistor breakdown field was not more than 10%. The residual voltage ratio (K_R) was determined as the ratio of $E_{500\ \mathrm{A/cm^2}}/E_{1\ \mathrm{mA/cm^2}}$ from the impulse response of varistors according to IEC-61643-1-2005 Standard. The disruptive discharge current was estimated according to BS EN 60099-4:1993 Standard as the current at which varistor was physically damaged.

3. Results and discussion

Fig. 1 shows the XRD patterns of the four sintered samples SCNCrY–*x*Bi where $x = 0$, 0.05, 0.15, and 0.45. The XRD spectra indicate the existence of a single phase solid solution of additives in an SnO_2 matrix in the samples, except SCNCrY–0.45Bi, where a minute amount of the secondary phase Co_2SnO_4 is detected. The maximum of the relative density 99.2% has been observed for the sample SCNCrY–0.05Bi. With increasing amount of Bi_2O_3 additive the relative density is decreased to 97% for SCNCrY–0.45Bi sample (Table 1).

Fig. 2 shows the back-scattered electrons micrographs of bismuth-doped samples. There are no signs of secondary phases in the samples containing 0.05 and 0.15 mol% Bi_2O_3 (Fig. 2a and b). However, in SCNCrY–0.45Bi sample (Fig. 2c) dark grains of a

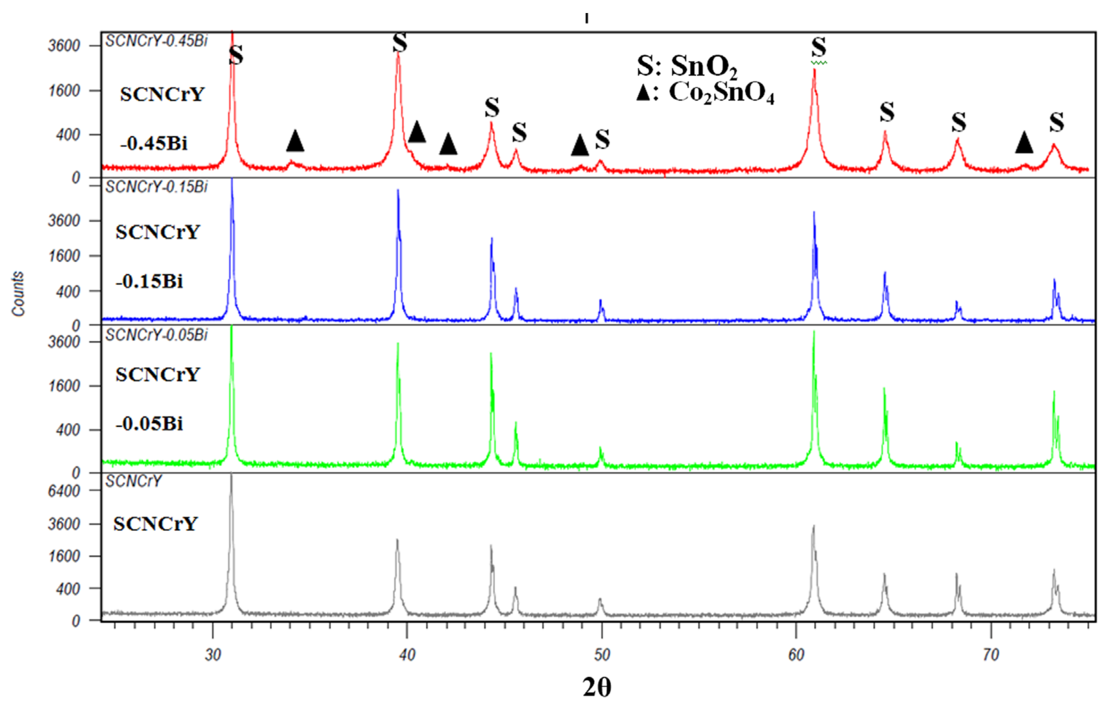

Fig. 1. X-ray diffraction patterns obtained from as-sintered Bi_2O_3-doped samples.

Table 1
Relative density, average grain size, and electrical parameters of studied Bi_2O_3-doped varistors.

	SCNCrY	SCNCrY-0.05Bi	SCNCrY-0.15Bi	SCNCrY-0.45Bi
Relative density (%)	98.5 ± 0.5	99.2 ± 0.5	98.1 ± 0.5	97.0 ± 0.5
Grain size (μm)	7 ± 1	10 ± 1	30 ± 3	42 ± 4
E_b (kV/cm)	2.2 ± 0.2	1.5 ± 0.2	0.5 ± 0.1	0.3 ± 0.05
α	37 ± 5	38 ± 5	22 ± 4	13 ± 3
I_L (μA)	15 ± 2	16 ± 2	33 ± 6	70 ± 10
Withstanding surge current (kA/cm^2)	2.5 ± 0.3	3 ± 0.3	2 ± 0.2	1 ± 0.2
K_R	2.2 ± 0.2	3.5 ± 0.2	5.8 ± 0.4	12 ± 0.9